

## How the Shape of the NH<sub>2</sub> Group Depends on the Substituent Effect and H-Bond Formation in Derivatives of Aniline

Halina Szatyłowicz\*

Faculty of Chemistry, Warsaw University of Technology, Noakowskiego 3, 00-664 Warsaw, Poland

Tadeusz M. Krygowski

Department of Chemistry, Warsaw University, Pasteura 1, 02-093 Warsaw, Poland

Pavel Hobza

Institute of Organic Chemistry and Biochemistry, Academy of Sciences of the Czech Republic, Flemingovo nam. 2, 16610 Prague 6, Czech Republic

Received: August 17, 2006; In Final Form: October 27, 2006

The geometry and electronic structure of the amino group in aniline and its derivatives are very sensitive to both intramolecular interactions such as substituent effects and intermolecular ones such as H-bonding. An analysis of experimental geometries retrieved from the CSD base and computational modeling of aniline and its derivatives and their H-bonded complexes by use of B3LYP/6-311+G\*\* and MP2/aug-cc-pVDZ showed that the degree of pyramidalization of the amino group depends on H-bonding, which exists in two forms, (i) NH $\cdots$ B (base) and (ii) N $\cdots$ HB (Brønsted acid), both of which affect the shape of the NH<sub>2</sub> group. The effect may be significantly enhanced by a substituent through resonance interaction from electron-attracting substituents. The NH $\cdots$ B interactions lead to a substantial planarization of the group, whereas N $\cdots$ HB interactions do not. The natural bond orbital analysis allowed the authors to show that the changes in occupancy of the “lone pair” orbital and in geometry parameters describing pyramidalization of the group depend on the substituent constants.

### Introduction

Ammonia, the mother compound of aniline, is a pyramidal molecule with a bond length of  $r(\text{N-H}) = 1.0124 \text{ \AA}$  and an HNH angle of  $106.67^\circ$ .<sup>1</sup> Replacement of one N-H bond by the N-C bond of a phenyl group leads to a decrease in pyramidalization and a slight shortening of the N-H bond length ( $r(\text{N-H}) = 1.001 \text{ \AA}$  and HNH angle  $113.1^\circ$ ).<sup>2</sup> These changes are due to a resonance effect between the lone pair at the NH<sub>2</sub> group and the  $\pi$ -electron system of the ring.<sup>3</sup> The geometry of the NH<sub>2</sub> group in aniline has been the subject of intensive studies, with a particular interest in its pyramidalization. A microwave study<sup>4</sup> yielded  $37.5^\circ \pm 2^\circ$  for the dihedral angle,  $\tau$ , between the plane of the amino group and the ring plane. This investigation was reanalyzed by Roussy and Nonat.<sup>5</sup> They found  $\tau = 42.4^\circ \pm 0.3^\circ$ , in agreement with the value measured by means of resonance fluorescence<sup>6</sup> and far-infrared<sup>7</sup> spectroscopies ( $\tau = 42^\circ$ ). A slightly larger value,  $44.30(16)^\circ$ , was derived from a semirigid bender analysis<sup>8</sup> of the far-infrared data.<sup>9</sup> Thoroughgoing analysis of gas-phase electron diffraction data and ab initio molecular orbital calculations at the HF and MP2 levels of theory yielded<sup>10</sup>  $44^\circ \pm 4^\circ$ ,  $41.8^\circ$ , and  $43.6^\circ$ , respectively. If the ring is linked in the *para* position to an electron-attracting group, say a nitro group,<sup>11</sup> a substantial intramolecular charge transfer takes place from the amino group through the ring to the nitro group. This transfer leads to changes

not only in the  $\text{p}K_{\text{a}}$  values of the amino group of substituted anilines but also in all geometry parameters and the charge distribution.<sup>12–14</sup> It results also in a nonadditivity of electric dipole moments and is associated with the changes in the spectral characteristics of the NH<sub>2</sub> group and practically all other parts of the system.<sup>15</sup> The influence of substituents on the structural parameters and cyclic  $\pi$ -electron delocalization in aromatic systems has recently become a subject of increased interest.<sup>16</sup>

Another important factor in determining the shape of the NH<sub>2</sub> group is its ability to interact by means of H-bond formation; two kinds of such interaction are possible,<sup>17,18</sup> (i) NH $\cdots$ B (base) and (ii) N $\cdots$ HB (Brønsted acid), and each of them not only may modify substantially the shape of the NH<sub>2</sub> group but also may affect a more distant part of the aniline derivatives involved in H-bonded complexes. If measurements are carried out in the condensed phase, then apart from the above-mentioned interaction types, there are also some other intermolecular interactions that may appear which will undoubtedly affect the geometry of the amine group. In the case of measurements in the crystalline state (X-ray or neutron diffraction) the interactions may be identified and roughly estimated as a source of geometry deformation.<sup>19</sup> A very good example of such interactions is a comparison of the geometry patterns of *p*-nitroaniline determined by X-ray diffraction<sup>20</sup> with the expected geometry built up from the gas-phase structure of aniline<sup>21</sup> and nitrobenzene.<sup>22</sup> Such a comparison shows how intermolecular interactions in the crystal lattice combined with intramolecular substituent effects influence the geometry of *p*-nitroaniline.

\* To whom correspondence should be addressed. E-mail: halina@chemix.ch.pw.edu.pl. Fax: (+48) 22 628 27 41. Phone: (+48) 22 234 77 55.

The aim of this paper is to present how the various indicators of the geometry and electron structure of the amino group are affected by the intramolecular (substituent effects) and intermolecular (H-bonding) interactions.

### Methodology

Geometries of H-bonded complexes of variously substituted aniline derivatives with various oxygen and nitrogen acids/bases were retrieved from CSD<sup>23</sup> with the following restrictions.

(1) The searches were performed for substituted aniline interacting with a nitrogen or oxygen base/acid with an intermolecular contact between the nitrogen of aniline and the nearest O or N atom in the base/acid equal to or less than the sum of their van der Waals radii.<sup>24</sup>

(2) The searches were restricted to structure measurements with the reported mean estimated standard deviation (esd) of the CC bond equal to or less than 0.005 Å, not disordered, without errors,  $R \leq 0.05$ , and 3D coordinates determined. The data were retrieved for polysubstituted aniline (by any of the following substituents: halogen, -Me, -CN, -COOH, -COO<sup>-</sup>, -COOMe, -COOEt, -CONH<sub>2</sub>, -CF<sub>3</sub>, -NH<sub>2</sub>, -NH<sub>3</sub><sup>+</sup>, -NO<sub>2</sub>, -OH, -OMe, -SO<sub>3</sub><sup>-</sup>, -H) interacting with N or O atom in the acid/base partner. Sometimes molecules of the solvent were also present in the crystal lattice.

The Becke-style three-parameter density functional method using the Lee–Yang–Parr correlation functional<sup>25</sup> with the 6-311+G\*\* basis set (B3LYP/6-311+G\*\*) and the second-order Moller–Plesset perturbation method<sup>26</sup> with the Dunning basis set<sup>27</sup> aug-cc-pVDZ (MP2/aug-cc-pVDZ) were used to optimize the molecules' geometries. The MP2 method when combined with an extended basis set such as the aug-cc-pVDZ ones yields reliable structures and energies of isolated systems as well as complexes. Contrary to DFT calculations the MP2 procedure also covers the dispersion energy, which might play an important role in stabilizing molecular clusters. On the other hand, an important advantage of the DFT method (over the MP2 ones) is that it can be used in combination with NBO analysis. To cover the geometrical features, the DFT calculations should be performed with basis set containing diffuse functions. In H-bonded complexes the linearity of N...H...B was assumed. Gaussian NBO,<sup>28</sup> version 3.1, for B3LYP/6-311+G\*-optimized molecules and complexes was utilized. All calculations were performed using the Gaussian03<sup>29</sup> series of programs.

### Results and Discussion

Figure 1 presents the dependence of the dihedral angle  $\Phi$ , defined as the angle between the H<sub>(1)</sub>NC<sub>(1)</sub> and H<sub>(2)</sub>NC<sub>(1)</sub> planes (see Chart 1 for labeling), on the CN bond length,  $d_{\text{CN}}$ , for experimental data retrieved from CSD<sup>23</sup> and modeled data computed at the B3LYP/6-311+G\*\* and MP2/aug-cc-pVDZ levels of theory. The CN bond length may be considered as an approximate measure of interactions between the lone pair at the nitrogen atom and the  $\pi$ -electron structure of the ring. The shorter the CN bond, the closer the electron structure at the nitrogen atom to sp<sup>2</sup> hybridization.

The most important result presented in Figure 1 is the good qualitative agreement between the plots for X-ray diffraction data (CSD<sup>23</sup>) and those modeled by DFT at the B3LYP/6-311+G\*\* level and MP2/aug-cc-pVDZ method. Moreover, the findings of the latter ones (i.e., both computational methods) are also in good qualitative agreement with each other.

The experimental data (Figure 1a) embrace variously substituted aniline derivatives (102 molecules) measured in a crystalline state. Due to that, a variety of intermolecular

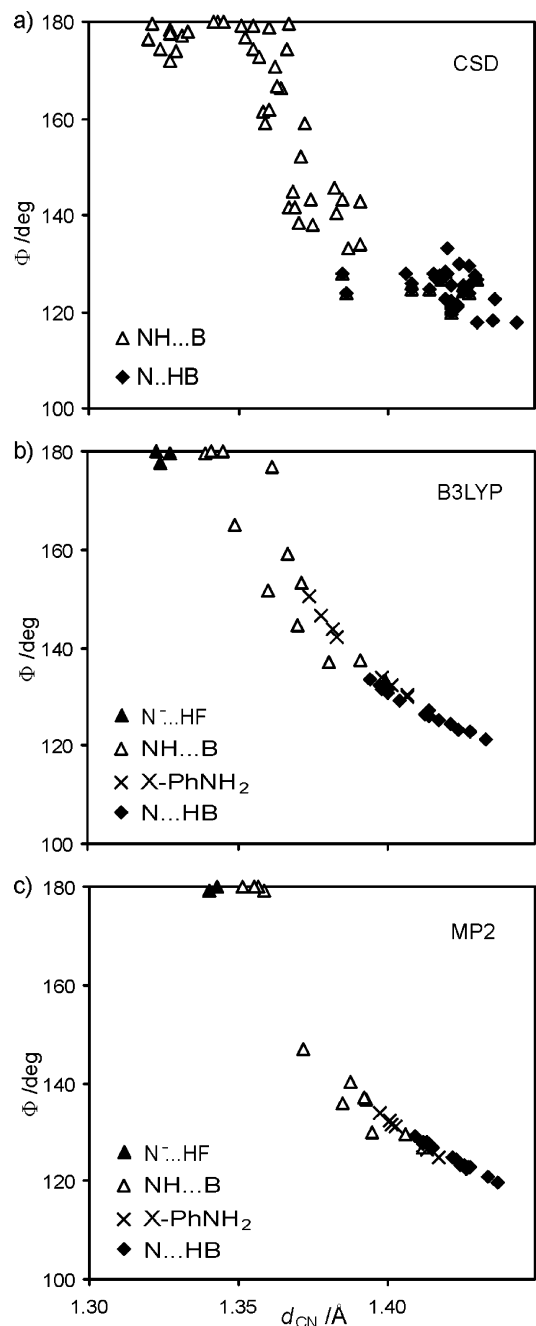
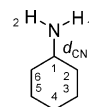


**Figure 1.** Dependences of the dihedral angle  $\Phi$  on the CN bond lengths,  $d_{\text{CN}}$ , for (a) experimental data (CSD<sup>23</sup>) and (b, c) optimized molecules of *p*-X-aniline (X = NO, NO<sub>2</sub>, CN, CHO, H, CH<sub>3</sub>, OCH<sub>3</sub>, OH) and its (X = NO, NO<sub>2</sub>, CHO, H, OH) derivatives involved in H-bond complexation computed at the (b) B3LYP/6-311+G\*\* and (c) MP2/aug-cc-pVDZ levels of theory.

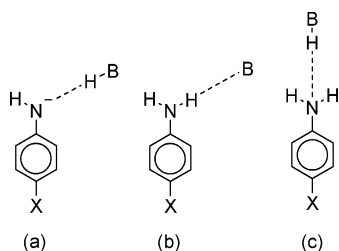
### CHART 1



$$\Sigma = H_{(1)}\text{NC}_{(1)} + H_{(2)}\text{NC}_{(1)} + H_{(1)}\text{NH}_{(2)}$$

$$\Phi = \text{angle between the planes defined by } H_{(1)}\text{NC}_{(1)} \text{ and } H_{(2)}\text{NC}_{(1)}$$

interactions (so-called crystal packing forces) operate, and hence, some deformations may occur. Additionally X-ray measurements are known for imprecision in the location of hydrogen. These effects may be a reason for a remarkable dispersion of the data in Figure 1a. Two main interactions between the NH<sub>2</sub>

CHART 2.<sup>a</sup>

<sup>a</sup> X = NO, NO<sub>2</sub>, CHO, H, OH.

group were identified: (i) NH<sup>+</sup>···B interactions in aniline derivatives (B is the Brønsted base), (ii) N<sup>+</sup>···HB interactions in aniline derivatives (HB is a Brønsted acid). In cases i and ii the lone pair of the nitrogen atom is indirectly (i) or directly (ii) involved in H-bond formation and is affected by electron-attracting substituents. Note that the greatest range for both the CN bond length (~1.32–1.43 Å) and the dihedral angle (180–120°) is observed for case i type interactions. The lengthening of the N–H bond as a result of H-bond formation makes the lone pair more mobile, and hence, a stronger substituent effect is observed from the electron-withdrawing group(s), which in turn leads to CN bond shortening. A reverse situation occurs in case ii; H-bond formation diminishes the mobility of the lone pair, and hence, a weaker substituent effect is observed for these systems. As a consequence, the range of changes in the CN bond length is substantially smaller, leading to considerably smaller changes in the dihedral angle (~1.39–1.44 Å and 133–118°, respectively).

The scatter plot based on experimental data (Figure 1a) is well supported by computation modeling (Figure 1b,c). The substituents selected for this study cover almost the whole set of classical substituents, embracing a wide range of intramolecular charge-transfer effects: from the strongly electron-attracting (NO<sub>2</sub>, NO, CHO) to typical electron-donating (OH, OMe) ones. To model H-bond formation, we accepted the idea<sup>30</sup> that the O<sup>-</sup>/OH groups in the phenol/phenolate system interacting with F<sup>-</sup> or HF are replaced by NH<sub>2</sub> in aniline derivatives interacting with B (B = F<sup>-</sup>, CN<sup>-</sup>, OH<sub>2</sub>) or HB (HB = HF, HCN, HOH), as shown in Chart 2. In the gas phase (computational modeling) a third type of H-bonding interaction of the amino group, N<sup>-</sup>···HB, was taken into account. The geometry was taken from equilibrium complexes schematically shown in Chart 2, for which the frequencies were positive.

B approaching H along the straight line elongated from the N–H bond (Chart 2b) simulates an increase of the strength of the H-bond of the type NH<sup>+</sup>···B, whereas HB approaching along the line characteristic of the lone pair (Chart 2c) models the interaction for aniline as a base in the H-bonding complex. In the first case, for 4-XPhNH<sub>2</sub>, where X = NO, NO<sub>2</sub>, CHO and B = F<sup>-</sup>, approaching F<sup>-</sup> toward H along the straight line causes proton transfer, and the complex 4-XPhNH<sup>+</sup>···HF is formed.

For some interatomic distances an equilibrium state is formed for which the dihedral angles,  $\Phi$ , and CN bond lengths,  $d_{\text{CN}}$ , are used (Figure 1b,c). The above-mentioned characteristics found for experimental data are supported by modeling. Again, the NH<sup>+</sup>···B interactions bear the greatest range of the dihedral angle (180–133° from B3LYP and 180–127° from MP2), and the dihedral angle for the N<sup>+</sup>···HB interactions (134–119° and 129–120° from B3LYP and MP2, respectively) are much smaller.

Another approach to describe the shape of the NH<sub>2</sub> group is based on estimating the sum of the bond angles,  $\Sigma$ , for bonds linking the nitrogen atom to two H atoms and to the carbon.

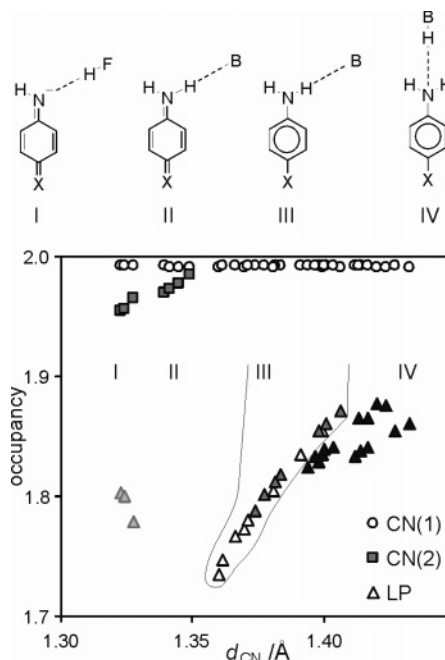


**Figure 2.** Dependence of the occupancies of the CN  $\sigma$  bond (CN(1), empty circles), the  $\pi$  contribution to the CN bond (CN(2), gray squares), and the free  $sp^2/sp^3$  orbital of the nitrogen, called the LP (triangles), on the CN bond length,  $d_{\text{CN}}$ , for B3LYP/6-311+G\*\* optimized molecules of *p*-X-aniline (gray triangles) and its derivatives involved in H-bond complexation: N<sup>-</sup>···HF (light-gray triangles), NH<sup>+</sup>···B (empty triangles), and N<sup>+</sup>···HB (black triangles); (I) X = NO, NO<sub>2</sub>, CHO; (II) X = H and B = F<sup>-</sup>; X = NO, NO<sub>2</sub>, CHO and B = CN<sup>-</sup>; (III) X = OH and B = F<sup>-</sup>; X = H, OH and B = CN<sup>-</sup>; X = NO, NO<sub>2</sub>, CHO, H, OH and B = OH<sub>2</sub>; *p*-X-aniline; (IV) *p*-XPhNH<sub>2</sub>···HB.

For the planar NH<sub>2</sub> group  $\Sigma = 360^\circ$ , and for ammonia  $\Sigma = 319.01^\circ$ ,<sup>1</sup> whereas for aniline  $\Sigma = 339.3^\circ$ .<sup>2</sup> Pyramidalization of the NH<sub>2</sub> group is associated with a decrease of the  $\Sigma$  value, indicating a change from  $sp^2$  hybridization of the nitrogen atom toward  $sp^3$ . On the other hand, these changes should be associated with a lengthening of the CN bond. Figure S1 (in the Supporting Information) presents these dependences for both experimental (Figure S1a) and modeled (Figure S1b,c) data.

Very good agreement between the experimental and theoretical data is additionally illustrated by scatter plots in Figure S2 (for X-ray data and modeling data, in the Supporting Information), where mutual dependences of  $\Sigma$  on the dihedral angle,  $\Phi$ , are shown. We are aware of the fact that  $\Phi$  and  $\Sigma$  are geometrically interrelated, but the point is how these scatter plots resemble each other, independently of the data, whether they come from computational optimization or from experiment.

The results presented in Figures 1 and S1 are fully supported by NBO<sup>28</sup> analysis of the occupancy at the “lone pair” (LP) orbital of the nitrogen atom and at CN bonds (CN(1) and CN(2)). Figure 2 shows the above-mentioned occupancies as a function of the CN bond length.

The data presented in Figure 2 allow one to find some concluding diversification.

(a) The occupancy of the  $\sigma$  orbital of the CN bond, labeled as CN(1), is practically independent of the CN bond length with a mean value of 1.992 and very little dispersion (standard deviation equal to 0.0003).

(b) The occupancy of the  $\pi$ -orbital contributing to the CN bond, labeled as CN(2), appears only for very short CN bonds (<1.35 Å). In these cases the  $\pi$ -orbital of the CN bond is characterized by a high occupancy (>1.95). Two subgroups can

be seen: with and without an LP (which is involved in H-bonding with HB) at the nitrogen atom for the lower and higher occupancy  $\pi$ -orbital (Figure 2, I and II), respectively. The first subgroup contains  $p$ -XPhNH<sup>-</sup>...HF complexes, where X = NO, NO<sub>2</sub>, and CHO. The second one includes H-bonded complexes:  $p$ -XPhNH<sub>2</sub>...CN<sup>-</sup> (X = NO, NO<sub>2</sub>, and CHO) and PhNH<sub>2</sub>...F<sup>-</sup>.

(c) For a CN bond length longer than 1.35 Å the occupancy for the  $\pi$ -bond orbital disappears and an occupancy of the LP orbital appears.

In the last case three subgroups may be distinguished. One of them consists of *para*-substituted aniline (Figure 2, LP, gray triangles). Another subgroup is formed by data for H-bonded complexes with NH...B interactions (empty triangles). These data form a clearly monotonic sequence with the lowest occupancy (~1.73) for the shortest CN bond (~1.36 Å), when the base is relatively weak or the electron-withdrawing power of the substituent is not too strong (e.g., in the case of *p*-hydroxyaniline...F<sup>-</sup>), in Figure 2 labeled as III. One more subgroup is formed by H-bonded complexes with N...HB interactions, labeled by black triangles (Figure 2, IV). It may be further divided into two subgroups: one when HB is hydrofluoric acid (the lower subgroup, i.e., the one with relatively long CN bonds) and the other for H-bonded complexes with hydrocyanic acid and water.

The results of geometry and occupancy studies lead to a consistent view confirming the opinion that the stronger the through-resonance (intermolecular charge transfer) of the NH<sub>2</sub> group with a counter substituent, and the more the N-H bond is involved in H-bonding with bases, the more planar the NH<sub>2</sub> group. For a CN bond length shorter than 1.35 Å there appears a high occupancy of the  $\pi$ -orbital of this bond.

**Analysis of the Dependences of the Geometry and NBO Parameters on the Substituent Constants.** The Hammett-type approach is a well-known empirical way of estimating the electronic influence of a substituent on the reaction site or another functional group.<sup>31</sup> This influence is numerically expressed by substituent constants  $\sigma$ , defined in most cases for disubstituted benzene derivatives.<sup>16,32</sup> Following Hammett's own citation, "substituent constants  $\sigma$  measure a change in electron density produced by substituent",<sup>31a</sup> it is reasonable to employ this kind of consideration in our case. Since our "reaction site", i.e., the functional group at which the changes are studied, is an electron-donating group, the modified Hammett constants  $\sigma_p^-$  have to be used.<sup>32c</sup>

Figure 3a presents a scatter plot of the occupancy of the lone pair orbital versus  $\sigma_p^-$ . It is clear that the data for *para*-substituted aniline derivatives (times signs) and H-bonded complexes of *para*-substituted aniline derivatives with bases (N...HB interactions, diamonds) follow a linear relation with  $cc = -0.996$  and  $cc = -0.960$ , respectively. For the NH...B interactions (triangles) a linear dependence exists only for B = H<sub>2</sub>O (empty triangles), with  $cc = -1.0$ . For two other bases, CN<sup>-</sup> and F<sup>-</sup>, no clear relation is observed at first sight, but it becomes evident if one looks at the occupancies of the CN bonds and the lone pair for the CN bond length in the range 1.32–1.38 Å (see Figure 2). In this range of CN bond length three different cases are observed (Figure 2, I–III): the lone pair and  $\pi$ -orbital of CN bond (I), only the  $\pi$ -orbital (II), and the case when the  $\pi$ -orbital disappears and there a lone pair orbital appears (III). Note that most sensitive is the occupancy at the lone pair orbital of the nitrogen for the NH...B interaction whereas the least sensitive is that for N...HB. The nonintermolecular interacting *para*-substituted anilines are in between.

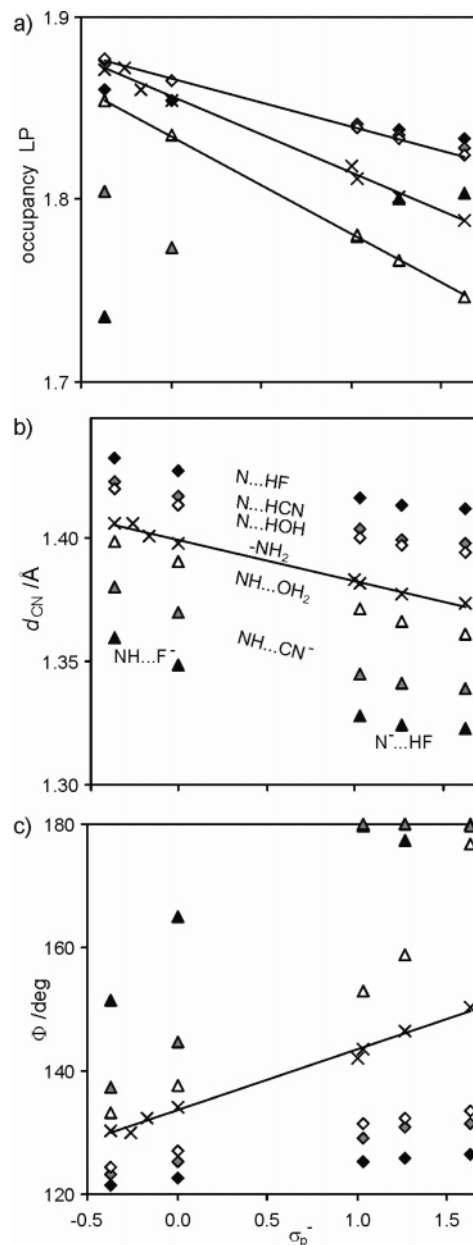


**Figure 3.** Dependence of (a) the occupancies at the lone pair orbital of the nitrogen atom, (b) the CN bond length,  $d_{\text{CN}}$ , and (c) the dihedral angle  $\Phi$  for B3LYP/6-311+G\*\*<sup>-</sup>-optimized molecules of *p*-X-aniline (times signs) and its derivatives involved in H-bond complexation, N...HF, NH...B, and N...HB, on the substituent constant  $\sigma_p^-$ . Black triangles and diamonds stand for B = F<sup>-</sup> and HB = HF, gray symbols for B = CN<sup>-</sup> and HB = HCN, and empty symbols for B = HB = OH<sub>2</sub>.

If geometry-based parameters of the NH<sub>2</sub> group are plotted against substituent constants, we find good linear relationships. Figure 3b presents such a linear relationship for the CN bond length plotted against  $\sigma_p^-$  for all the systems studied. A general trend, i.e., linear regressions with negative slopes, is understandable; the stronger the through-resonance effect, the shorter the CN bond. Interpretation of the intercept is also clear. The intercept is the highest for N...HB systems in which the lone pair electrons are involved in attractive interactions via H-bonding with HB. This means that they are less mobile, and hence, the bond is longer. The intercept of the regression for free (no intermolecular interactions) *para*-substituted aniline derivatives has a substantially lower value; in this case the lone pair is involved only in intramolecular charge transfer associated



with an increase of a quinoid structure weight with an increase of the electron-attracting power of the substituent, i.e., an increase in the magnitude of  $\sigma_p^-$ . The values of the intercept for the systems with  $\text{NH}\cdots\text{B}$  interactions are much lower. Moreover, their values are more differentiated. The lower value is for  $\text{F}^-$ , then for  $\text{CN}^-$ , and the highest one is for water as a base. The lowest value of the intercept is for complexes of the type  $\text{N}^-\cdots\text{HF}$ .

Figures 3c and S3 (in the Supporting Information) present parameters of deviation from planarity of the  $\text{NH}_2$  group ( $\Sigma$  and dihedral angle  $\Phi$ ) plotted against  $\sigma_p^-$ . In both cases, except the data for free *para*-substituted aniline derivatives and weakly interacting H-bonded systems with water as a base, the regression lines are steeper for lower values of the substituent constants, and less steep or even flat for the higher values of  $\sigma_p^-$ . This is most convincing for strongly interacting  $\text{NH}\cdots\text{B}$  systems with  $\text{B} = \text{CN}^-$ . For strongly electron-attracting substituents ( $\text{NO}_2$ ,  $\text{CHO}$ , and  $\text{CN}$ ), if  $\text{B} = \text{F}^-$ , proton transfer to the base and anilide anion is formed (Chart 2a).

## Conclusion

The shape of the  $\text{NH}_2$  group of aniline derivatives depends on the substituent (intramolecular interaction) and intermolecular interaction by H-bonding, in which the nitrogen could be both the proton donor and the proton acceptor. Both the theoretically and experimentally obtained structural parameters for aniline and its substituted derivatives and complexes with H-bonding show a coherent view. A decrease in pyramidalization of the  $\text{NH}_2$  group is nicely related to (i) an increase of the  $\pi$ -electron-accepting power of the *para*-substituent (substituent effect quantified by  $\sigma_p^-$ ) and (ii) the H-bonding complexation,  $\text{NH}\cdots\text{B}$  and  $\text{N}\cdots\text{HB}$ , the power of interaction of which is approximately described by the  $\text{N}-\text{H}$  or  $\text{N}\cdots\text{H}$  interatomic distance. The analysis based on geometrical parameters leads to the same picture as that obtained by NBO studies. If the changes in pyramidalization are considered as a result of the substituent effect, then the range of variation (for  $\Phi$  it is  $\sim 20^\circ$  and  $9^\circ$  from B3LYP and MP2 calculations, respectively) is significantly smaller than in the case in which we have included intermolecular H-bonding (for  $\text{NH}\cdots\text{B}$ , ca.  $47^\circ$  and  $53^\circ$  and, for  $\text{N}\cdots\text{HB}$ ,  $\sim 12^\circ$  and  $9^\circ$ , B3LYP and MP2, respectively). The range of variation of  $\Phi$  in aniline H-bonded complexes of the  $\text{NH}\cdots\text{B}$  type is ca.  $27^\circ$  and  $49^\circ$  and that for the  $\text{N}\cdots\text{HB}$  type  $\sim 4^\circ$  and  $4^\circ$  (B3LYP and MP2, respectively). This is due to the increase of the donating power of the nitrogen if the amino group is involved in H-bonding. Which interactions, intra- or intermolecular, have “more power”? The answer is not surprising; small is powerful, particularly when the amino group acts as a proton donor in H-bonded complexes.

**Note Added in Proof.** A similar problem of the shape of the  $\text{NH}_2$  group, in triazine-based derivatives, has been recently discussed by Fernandez et al., *Chem. Phys. Lett.* **2006**, *426*, 290–295.

**Acknowledgment.** This paper is dedicated to Prof. Bogdan Marciniak (UAM, Poznan) on the occasion of his 65th birthday. We thank the Interdisciplinary Center for Mathematical and Computational Modeling (Warsaw, Poland) for use of their computational facilities and the Warsaw University of Technology for financial support.

**Supporting Information Available:** Figure S1, dependence of  $\Sigma$  on the CN bond lengths for experimental and modeling

data, Figure S2, dependence of  $\Sigma$  on the dihedral angle  $\Phi$  for experimental and modeling data, Figure S3, dependence of  $\Sigma$  on the substituent constant  $\sigma_p^-$ , and Table S1, comparison of the results of B3LYP/6-311+G\*\* and MP2/aug-cc-pVDZ calculations (CN bond length, dihedral angle  $\Phi$ , and the sum of the bond angles  $\Sigma$ ). This material is available free of charge via the Internet at <http://pubs.acs.org>.

## References and Notes

- (1) *Tables of Interatomic Distances and Configuration in Molecules and Ion*; Sutton, L. E., Ed.; The Chemical Society: London, 1958; p 385; Supplement, 1965; p 288.
- (2) *Molecular Structure by Diffraction Methods*; Sim, G. A., Sutton, L. E., Eds.; The Chemical Society: London, 1973; Vol. 1; 1974; Vol. 2; 1975; Vol. 3; 1976; Vol. 4; 1977; Vol. 5; 1978; Vol. 6.
- (3) (a) Vollhardt, K. P. C.; Schore, N. E. *Organic Chemistry: Structure and Function*; W. H. Freeman and Co.: New York, 1998. (b) Smith, M. B.; March, J. *March's Advanced Organic Chemistry*, 5th ed.; J. Wiley: New York, 2001. (c) Pine, S.; Hendricson, J. B.; Cram, D. J.; Hammond, G. S. *Organic Chemistry*, 4th ed.; McGraw-Hill: New York, 1980.
- (4) Lister, D. G.; Tyler, J. K.; Hog, J. H.; Larsen, N. W. *J. Mol. Struct.* **1974**, *23*, 253–264.
- (5) Roussy, G.; Nonat, A. *J. Mol. Spectrosc.* **1986**, *118*, 180–188.
- (6) Quack, M.; Stockburger, M. *J. Mol. Spectrosc.* **1972**, *43*, 87–116.
- (7) Larsen, N. W.; Hansen, E. L.; Nicolaisen, F. M. *Chem. Phys. Lett.* **1976**, *43*, 584–586.
- (8) Kleibomer, B.; Sutter, D. H. *Z. Naturforsch., Teil A* **1988**, *43*, 561.
- (9) Kydd, R. A.; Krueger, P. J. *Chem. Phys. Lett.* **1977**, *49*, 539–543.
- (10) Schultz, G.; Portalone, G.; Ramondo, F.; Domenicano, A.; Hargittai, I. *Struct. Chem.* **1996**, *7*, 59–71.
- (11) Exner, O.; Krygowski, T. M. *Chem. Soc. Rev.* **1996**, *25*, 71–75.
- (12) (a) Gross, K. C.; Seybold, P. G. *Int. J. Quantum Chem.* **2000**, *80*, 1107–1115. (b) Gross, K. C.; Seybold, P. G.; Hadad, C. M. *Int. J. Quantum Chem.* **2002**, *90*, 445–458. (c) Vaschetto, M. E.; Retamal, B. A.; Monkman, A. P. *J. Mol. Struct.: THEOCHEM* **1999**, *468*, 209–221. (e) Wojciechowski, P. M.; Zierkiewicz, W.; Michalska, D.; Hobza, P. *J. Chem. Phys.* **2003**, *118*, 10900–10911. (f) Palafox, M. A.; Gill, M.; Nunez, N. J.; Rastogi, V. K.; Mittal, L.; Sharma, R. *Int. J. Quantum Chem.* **2005**, *103*, 394–421.
- (13) Bartmess, J. E.; Scott, J. A.; McIver, R. T., Jr. *J. Am. Chem. Soc.* **1979**, *101*, 6046–6056.
- (14) Hillebrand, C.; Klessinger, M.; Eckert-Maksic, M.; Maksic, Z. B. *J. Phys. Chem.* **1996**, *100*, 9698–9702.
- (15) (a) *The chemistry of amino, nitroso and nitro compounds and their derivatives*; Patai, S., Ed.; J. Wiley: New York, 1982; Part I, Suppl. F. (b) *The chemistry of amino, nitroso and nitro compounds and their derivatives*; Patai, S., Ed.; J. Wiley: New York, 1996; Part I, Suppl. F2.
- (16) For a review, see: Krygowski, T. M.; Stępień, B. T. *Chem. Rev.* **2005**, *105*, 3482–3512.
- (17) Szatyłowicz, H.; Krygowski, T. M.; Zachara, J. E. To be published.
- (18) Sobczyk, L.; Grabowski, S. J.; Krygowski, T. M. *Chem. Rev.* **2005**, *105*, 3513–3560.
- (19) Bernstein, J. In *Accurate Molecular Structures—Their Determination and Importance*; Domenicano, A., Hargittai, I., Eds.; Oxford University Press: Oxford, U.K., 1992; Chapter 19, p. 469.
- (20) Colapietro, M.; Domenicano, A.; Marciantie, C.; Portalone, G. *Z. Naturforsch.* **1982**, *37b*, 1309–1311.
- (21) (a) Lister, D. G.; Tyler, J. K.; Hog, J. H.; Larsen, N. W. *J. Mol. Struct.* **1974**, *23*, 253–264. (b) Schultz, G.; Portalone, G.; Ramondo, F.; Domenicano, A.; Hargittai, I. *Struct. Chem.* **1996**, *7*, 59–71.
- (22) Domenicano, A.; Schultz, G.; Hargittai, I.; Colapietro, M.; Portalone, G.; George, P.; Bock, C. W. *Struct. Chem.* **1990**, *1*, 107–120.
- (23) *The Cambridge Structure Database*, 5.27 version; The Cambridge Crystallographic Data Centre: Cambridge, U.K., November 2005, updated January 2006.
- (24) Bondi, A. *J. Phys. Chem.* **1964**, *68*, 441–451.
- (25) (a) Lee, C.; Yang, W.; Parr, R. G. *Phys. Rev. B* **1988**, *37*, 785–789. (b) Becke, A. D. *J. Phys. Chem.* **1993**, *98*, 1372–1377. (c) Becke, A. D. *J. Chem. Phys.* **1993**, *98*, 5648–5662. (d) Stephens, P. J.; Devlin, F. J.; Chabalowski, C. F.; Frisch, M. J. *J. Phys. Chem.* **1994**, *98*, 11623–11627.
- (26) (a) Moller, C.; Plesset, M. S. *Phys. Rev.* **1934**, *46*, 618–622. (b) Krishnan, R.; Pople, J. A. *Int. J. Quantum Chem.* **1978**, *14*, 91–100.
- (27) (a) Dunning, T. H., Jr. *J. Chem. Phys.* **1989**, *89*, 1007–1023. (b) Kendall, R. A.; Dunning, T. H., Jr.; Harrison, R. J. *J. Chem. Phys.* **1992**, *96*, 6796–6806. (c) Woon, D. E.; Dunning, T. H., Jr. *J. Chem. Phys.* **1993**, *98*, 1358–1371.
- (28) (a) Foster, J. P.; Weinhold, F. *J. Am. Chem. Soc.* **1980**, *102*, 7211–7218. (b) Reed, A. E.; Weinhold, F. *J. Phys. Chem.* **1983**, *78*, 4066–4073. (c) Reed, A. E.; Weinstock, R. B.; Weinhold, F. *J. Phys. Chem.* **1985**, *83*, 735–746. (d) Reed, A. E.; Weinhold, F. *J. Phys. Chem.* **1985**, *83*, 1736–

1740. (e) Carpenter, J. E.; Weinhold, F. *J. Mol. Struct.: THEOCHEM* **1988**, *169*, 41–62. (f) Reed, A. E.; Curtis, L. A.; Weinhold, F. *Chem. Rev.* **1988**, *88*, 899–926.

(29) Frisch, M. J.; Trucks, G. W.; Schlegel, H. B.; Scuseria, G. E.; Robb, M. A.; Cheeseman, J. R.; Montgomery, J. A., Jr.; Vreven, T.; Kudin, K. N.; Burant, J. C.; Millam, J. M.; Iyengar, S. S.; Tomasi, J.; Barone, V.; Mennucci, B.; Cossi, M.; Scalmani, G.; Rega, N.; Petersson, G. A.; Nakatsuji, H.; Hada, M.; Ehara, M.; Toyota, K.; Fukuda, R.; Hasegawa, J.; Ishida, M.; Nakajima, T.; Honda, Y.; Kitao, O.; Nakai, H.; Klene, M.; Li, X.; Knox, J. E.; Hratchian, H. P.; Cross, J. B.; Adamo, C.; Jaramillo, J.; Gomperts, R.; Stratmann, R. E.; Yazyev, O.; Austin, A. J.; Cammi, R.; Pomelli, C.; Ochterski, J. W.; Ayala, P. Y.; Morokuma, K.; Voth, G. A.; Salvador, P.; Dannenberg, J. J.; Zakrzewski, V. G.; Dapprich, S.; Daniels, A. D.; Strain, M. C.; Farkas, O.; Malick, D. K.; Rabuck, A. D.; Raghavachari, K.; Foresman, J. B.; Ortiz, J. V.; Cui, Q.; Baboul, A. G.; Clifford, S.; Cioslowski, J.; Stefanov, B. B.; Liu, G.; Liashenko, A.; Piskorz,

P.; Komaromi, I.; Martin, R. L.; Fox, D. J.; Keith, T.; Al-Laham, M. A.; Peng, C. Y.; Nanayakkara, A.; Challacombe, M.; Gill, P. M. W.; Johnson, B.; Chen, W.; Wong, M. W.; Gonzalez, C.; Pople, J. A. *Gaussian 03*, revision C.02; Gaussian, Inc.: Wallingford, CT, 2004.

(30) (a) Krygowski, T. M.; Zachara, J. E.; Szatyłowicz, H. *J. Phys. Org. Chem.* **2005**, *18*, 110–114. (b) Krygowski, T. M.; Szatyłowicz, H.; Zachara, J. E. *J. Chem. Inf. Comput. Sci.* **2004**, *44*, 2077–2082.

(31) (a) Hammett, L. P. *Physical Organic Chemistry*, 1st and 2nd eds.; McGraw-Hill: New York, 1940 and 1970. (b) Jaffe, H. H. *Chem. Rev.* **1953**, *53*, 191–261. (c) Johnson, C. D. *The Hammett Equation*; Cambridge University Press: Cambridge, U.K., 1973.

(32) (a) Charton, M. *Prog. Phys. Org. Chem.* **1981**, *13*, 119–251. (b) Exner, O. In *Correlation Analysis of Chemical Data*; Chapman, N. B., Shorter, J., Eds.; Plenum Press: New York, 1988; Chapter 10, p 439. (c) Hansch, C.; Leo, A.; Taft, R. W. *Chem. Rev.* **1991**, *91*, 165–195.